OAK RIDGE
NATIONAL LABORATORY

MANAGED BY UT-BATTELLE
FOR THE DEPARTMENT OF ENERGY

ORNL/TM-2000/316

COMPUTATION OF DETECTION EFFICIENCIES FOR NMIS FAST PLASTIC SCINTILLATORS USING A THICK DETECTOR MODEL

L. G. Chiang and R. B. Oberer

October 2000

Abstract

This report describes and compares the computation of the detection efficiencies for fast plastic scintillating detectors from their Time-of-Flight (TOF) spectrums using two different detector models. In the first method which assumes a thin detector model, a one-to-one correspondence between the energy of the neutron and the time bin in which it appears in the TOF spectrum is used in computing the detector efficiencies. In the second method which is based upon a thick detector model, the macroscopic cross sections of the detector materials are used to determine the path length of a neutron in the detector and hence its time of detection. With this model, neutrons of a given energy E_n, are distributed across several time bins in the TOF spectrum.

Contents

1 Setup for Computing Detector Efficiencies **1**

2 Thin Detector Model **2**

3 Thick Detector Model **6**

4 Conclusion **10**

1 Setup for Computing Detector Efficiencies

The detection efficiencies of the fast plastic scintillating detectors used in the Nuclear Materials Identification System (NMIS) can be computed from their Time-of-Flight (TOF) spectrums using *a priori* knowledge of the fission spectrum of the instrumented ^{252}Cf source. A typical setup for simultaneously measuring four detector efficiencies from their Time-of-Flight measurements is shown in Figure 1.

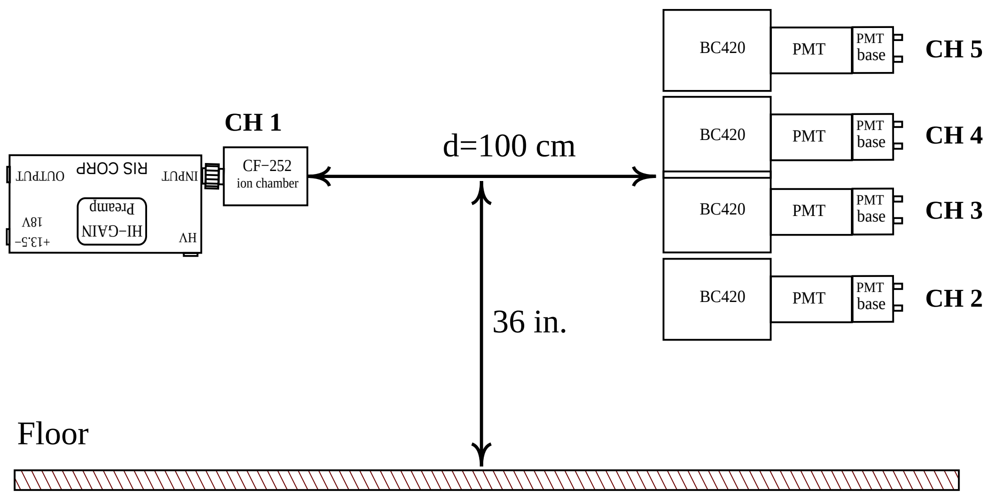

Figure 1: Side view of Time-of-Flight setup for NMIS.

Note that in this setup, a TOF spectrum corresponds to the source-detector correlation measured by NMIS [7] as shown in Figure 2. Notice that this spectrum has two prominent features, a sharp gamma peak followed by a broad neutron distribution. In Figure 2, all time lags are referenced to the detection of a source fission event at time lag 0. The gamma peak is sharp because all the gammas travel at the speed of light and thus reach the detector at a time corresponding to the source-detector distance. For a source-detector separation of 100 cm, the gamma peak appears at 3.3 ns in the TOF spectrum. The neutrons however, have a distribution of speeds as a direct result of their spectrum of emission energies from the fission process. This energy distribution leads to a broad time distribution of the neutrons in the TOF

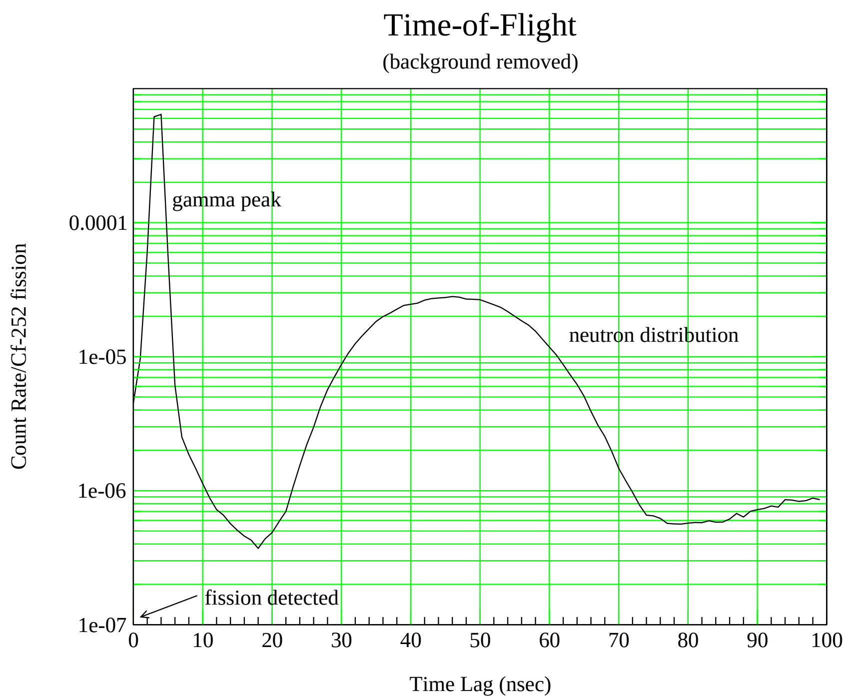

Figure 2: Source-detector correlation for source-detector distance of 100 cm.

spectrum. It is this energy and time dependence that permits the computation of the neutron detection efficiency from a TOF spectrum. Conversely, since no energy-time relationship exists for gammmas, a gamma detection efficiency can not be computed from the TOF spectrum.

2 Thin Detector Model

If the detector thickness is small with respect to the total source-detector separation distance, the detector efficiencies can be simply computed by dividing the measured neutron counts $C(t)$, in each time bin by the expected neutron counts, $N(E_n)$. The expected number in each time bin must correspond to the integral of the fission spectrum evaluated at the energy limits that correspond to the time bin limits. The expected counts $N(E_n)$, is also a function of the geometry factor and the average neutron multiplicity. This calculation is summarized below in Equation 1

$$N(E_1 < E_n < E_2) = S\,\overline{\nu}\,g \int_{E_1}^{E_2} \chi(E_n)\,dE_n \tag{1}$$

where

$\boldsymbol{E_n}$ is the neutron energy,

$\boldsymbol{S}$ is the detected fission rate of the instrumented $\boldsymbol{^{252}Cf}$ source,

$\boldsymbol{\overline{\nu}}$ is the average number of neutrons emitted per fission,

$\boldsymbol{g}$ is the geometry factor, and

$\boldsymbol{\chi(E_n)}$ is the neutron fission spectrum.

The energy limits, E_1 and E_2, in Equation 1 are computed using the nonrelativistic relationship between energy and mass,

$$\begin{aligned} E_1 &= \frac{1}{2}m\left(\frac{d}{t_1}\right)^2, \text{ and} \\ E_2 &= \frac{1}{2}m\left(\frac{d}{t_2}\right)^2. \end{aligned}$$

The fission spectrum, $\chi(E_n)$, for a nuclide with a nuclear temperature of T can be modeled by several different probability distribution functions. The Maxwellian distribution in Equation 2 and shown in Figure 3 is reasonably accurate

$$\chi(E_n) = \frac{2}{\sqrt{\pi}}\frac{\sqrt{E_n}}{T^{3/2}}e^{-\frac{E_n}{T}}. \tag{2}$$

For ^{252}Cf, T is 1.42 MeV. If this model of the fission spectrum is used in Equation 1, a closed form solution for this integral is

$$N(E_1 < E_n < E_2) = S\,\overline{\nu}\,g\left[erf\left(\sqrt{\frac{E_2}{T}}\right) - erf\left(\sqrt{\frac{E_1}{T}}\right) + T\left[\chi(E_2) - \chi(E_1)\right]\right]. \tag{3}$$

Assuming that the source is isotropic, the number of detector counts depends on the solid angle Ω, subtended by the front face of the detector at a distance d from the

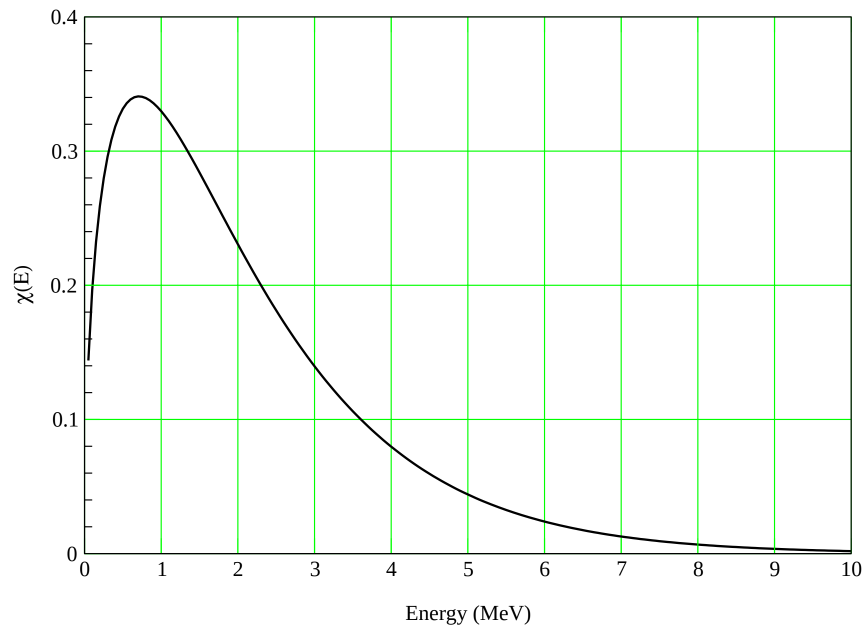

Figure 3: Maxwellian fission spectrum for ^{252}Cf.

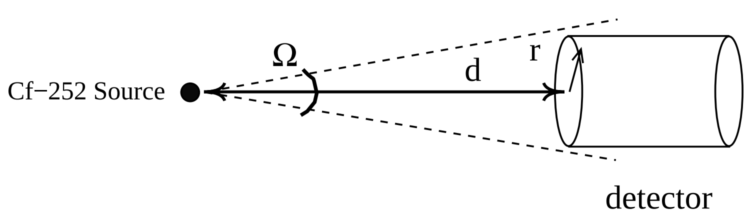

Figure 4: Isotropic source and solid angle subtended by right cylindrical detector.

source as shown in Figure 4. The geometry factor, g is proportional to Ω and can be computed by modeling the NMIS rectangular detector [4] as a right cylindrical detector that has the same volume and front surface area [6]. Thus, if the NMIS detector front face is a square with side s, then the radius of the equivalent right cylindrical detector can be computed using $r = s/\sqrt{\pi}$. Equation 4 can be used to compute the geometry factor,

$$g = \frac{1}{2}\left(1 - \frac{d}{\sqrt{d^2 + r^2}}\right) \tag{4}$$

where

d is the distance from the source to the detector's front face, and

r is the radius of the right cylindrical detector.

Using these formulas, the detector efficiency can be computed from an NMIS TOF measurement

$$\begin{aligned}\epsilon(E_n) &= \frac{\text{Measured counts}}{\text{Expected counts}} \times 100 \\ &= \frac{C(E_n)}{N(E_n)} \times 100 \end{aligned} \tag{5}$$

as shown in Figure 5.

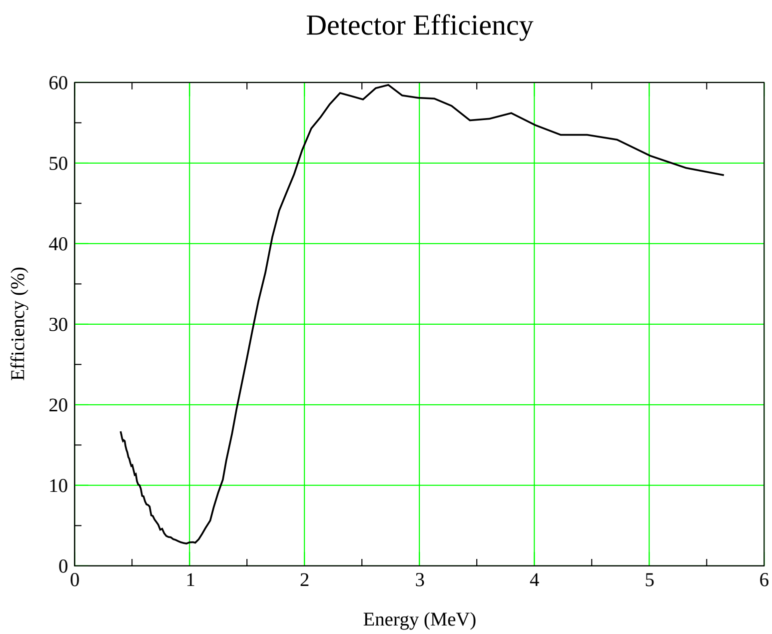

Figure 5: Detector efficiency computed from TOF using the thin detector model.

3 Thick Detector Model

The thin detector model assumes a one-to-one correspondence between the time of detection and the energy of the neutron. When a detector is thick enough that it takes more than one time bin for a neutron to traverse the detector the thin model no longer holds. A neutron will take a time $t_0 = d\sqrt{\frac{2E_n}{m}}$ to reach the front face of the detector. It will then take a time $t_l = l\sqrt{\frac{2E_n}{m}}$ to exit at the back of the detector. The neutron can therefore interact and register a count at any time between t_0 and $t_0 + t_l$. A plot of these two times as a function of neutron energy is shown in Figure 6. Figure 6 gives some indication of the joint probability distribution $p(t, E_n)$. We know

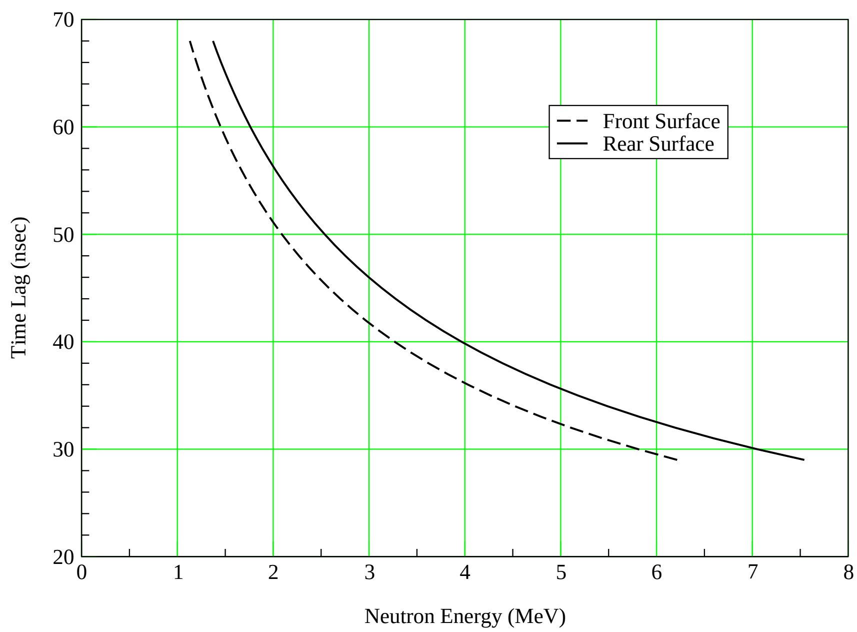

Figure 6: The time it takes a neutron to reach the front face of the detector and the time it takes to exit the detector as a function of neutron energy.

that it must be zero outside the two curves. For now we can continue the discussion without specifying $p(t, E_n)$.

The probability density $\chi(E_n)$ can be combined with the probability of the time of detection to form a detector response function:

$$R(t, E_n) = S\, g\, \overline{\nu}\, \chi(E_n) p(t, E_n) \tag{6}$$

where time t, velocity v, and energy E_n are related by

$E_n = \frac{1}{2} m v^2 = \frac{1}{2} m \left(\frac{d}{t_0}\right)^2$, and

$t = x\sqrt{\frac{2E_n}{m}}$.

The TOF spectrum is then

$$C(t) = \int_0^\infty \epsilon(E_n) R(t, E_n) dE_n \tag{7}$$

Of course NMIS integrates the detector response over individual time bins of width Δt, typically 1 ns. The result is a detector response matrix of the form

$$\overline{C_i(t)} = [R_{ij}]\, \overline{\epsilon_j(E_n)} \tag{8}$$

where the index i corresponds to time t and the index j corresponds to the neutron energy E_n. The matrix R_{ij} is square and invertible. The detector efficiency then, is determined by solving

$$\overline{\epsilon_j(E_n)} = [R_{ij}]^{-1}\, \overline{C_i(t)} \tag{9}$$

We now must return to the issue of specifying $p(t, E_n)$. Let's assume that the probability of a neutron reaching a distance x in the detector is given by $p(x) = \Sigma(E_n) e^{-\Sigma(E_n)x}$. This position is related to time by $x = v(t - t_0)$, where v is the velocity of the neutron, and t_0 is the time to the front face of the detector. The probability density[1] can therefore be written in terms of time as $p(t, E_n) = \Sigma(E_n) e^{-\Sigma(E_n) v(t-t_0)} U(t - t_0)$. In the case of a detector of thickness l, this probability density is truncated at $t_0 + t_l$, where $t_l = \frac{l}{v}$ is the time the neutron takes to traverse the detector. The probability density[2] then becomes $k e^{-\Sigma(E_n) v(t-t_0)} [U(t - t_0) - U(t - t_0 - t_l)]$. This truncated

[1] $U(t - t_0)$ is the unit step function which is used to limit the response to times, $t > t_0$

[2] $U(t - t_0) - U(t - t_0 - t_l)$ limits the response to times, $t_0 < t < t_l$

probability density function must be renormalized. The normalizing constant, k, can be computed by

$$k = \frac{\Sigma(E_n)}{1 - e^{-\Sigma(E_n)vt_0}}. \tag{10}$$

A few observations can be drawn from this probability density. First, the most probable depth of interaction is $x = 0$ which corresponds to t_0, i.e., the front face of the detector. The average depth of interaction is

$$\overline{x} = \frac{1}{\Sigma(E_n)} - \frac{le^{-\Sigma(E_n)l}}{1 - e^{-\Sigma(E_n)l}}. \tag{11}$$

The appropriate cross sections must be considered. The assumption is that the probability of detection depends on the probability of the neutron reaching a particular depth in the detector. One approach would be to use the total macroscopic cross section and assume that a single interaction removes the neutron from the system. The macroscopic cross section is related to the microscopic cross section by $\Sigma_i = N_i\sigma_i$ where σ_i is the microscopic cross section and N_i is the number density for the ith material. The total macroscopic cross section is the summation of all of the individual macroscopic cross sections. The NMIS plastic detectors (Bicron 420) are composed of hydrogen and carbon with number densities of 5.21×10^{-2} and $4.74\times10^{-2}/barn{-}cm^2$, respectively.

Figure 7 shows the carbon, hydrogen, and total macroscopic cross sections. Note that hydrogen has no large resonances whereas the carbon cross section does.

Substituting $p(t, E_n)$ into Equation 6 yields

$$R(t, E_n) = Sg\overline{\nu}\chi(E_n)ke^{-\Sigma(E_n)v(t-t_0)}[U(t - t_0) - U(t - t_0 - t_l)] \tag{12}$$

NMIS integrates the detector response over individual time bins of width Δt. This integration results in the response matrix

$$[R_{ij}] = \begin{cases} \chi_j ke^{-\Sigma(E)vi\Delta t}\left(1 - e^{-\Sigma(E)v\Delta t}\right) & \text{for } \frac{t_0}{\Delta t} \le i < \frac{t_0+t_l}{\Delta t} \\ \\ 0 & \text{otherwise.} \end{cases} \tag{13}$$

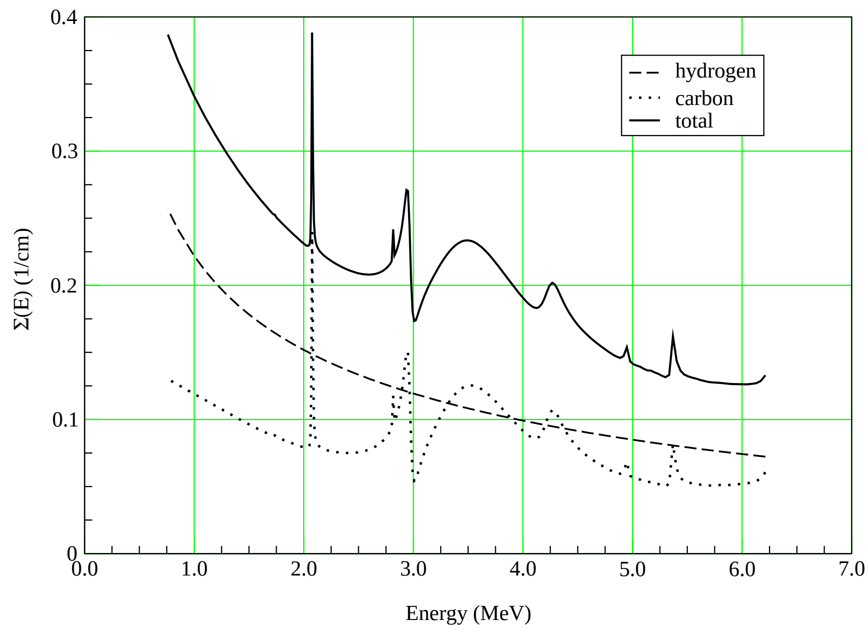

Figure 7: Macroscopic cross sections of carbon and hydrogen.

The variable χ_j is the integrated fission spectrum, evaluated between the energy limits that correspond to the time bin limits, i.e., $\chi_j = \int_{E_j-1}^{E_j} \chi(E)dE$.

A third case must also be considered for $\frac{t_0+t_l}{\Delta t} \leq i < \frac{t_0+t_l+\Delta t}{\Delta t}$. This third case occurs because the neutron does not traverse the detector in an integer number of time bins. Unlike t_0 which by definition begins the first time bin, the time at which the neutron exits the detector does not occur on a time bin boundary. A natural solution is to integrate over part of the final time bin as follows: $\chi_j k e^{-\Sigma(E)vi\Delta t}\left(1 - e^{-\Sigma(E)v(t_0+t_l-i\Delta t)}\right)$. Another approach is to integrate over the entire time bin if the time into the time bin is greater than $\frac{\Delta t}{2}$.

Six energy slices of the joint probability matrix $[R_{ij}]$ are shown in Figure 8. Note that for short time lags which correspond to high energy neutrons, the pdf falls off steeply and neutrons only appear in a few time bins. Conversely, at longer time lags

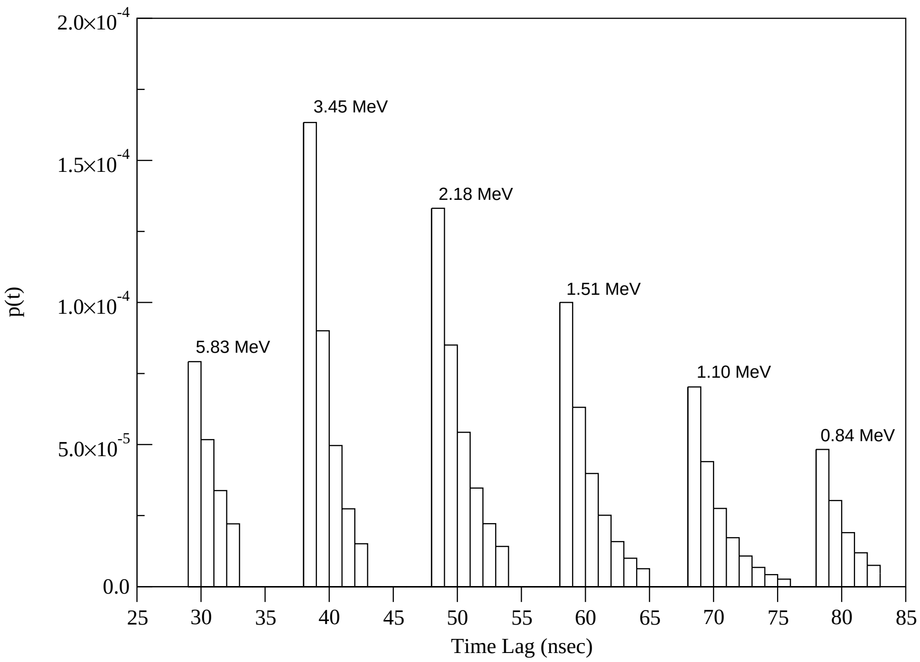

Figure 8: Six energy slices of R-matrix.

which correspond to lower energy neutrons, the pdf falls of less steeply and hence neutrons appear in more time bins.

A plot of the calculated detector efficiency for the TOF spectrum (see Figure 2) is shown in Figure 9. For comparison, the detector efficiency using the thin detector model is also shown. The thick detector model efficiencies approaches the thin model efficiencies as $t_l - t_0$ approaches Δ_t or as the total macroscopic cross section becomes very large.

4 Conclusion

Two models can be used to compute the detector efficiencies from their Time-of-Flight spectrums, a thin detector or a thick detector. If the detector depth is large compared

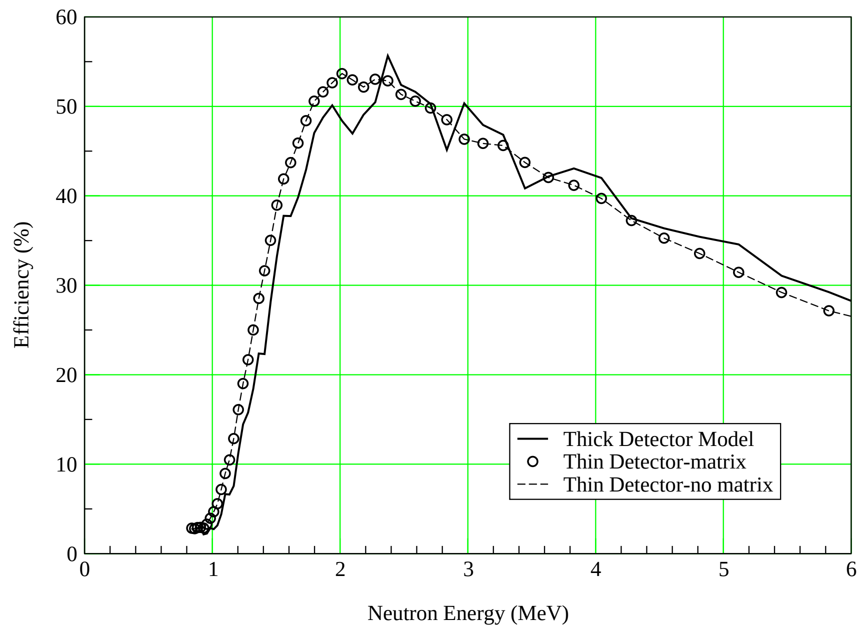

Figure 9: Comparison of detector efficiencies using thin and thick detector models.

to the source-detector distance, then the thick model should be used. One method to tell if the detector is thick, is to plot the probability density of the depth of interaction in terms of time for the highest neutron energy of interest. If the pdf exceeds more than one time bin, then the thick model should be used.

For the NMIS detectors, the detector is a thick detector for both low and high energy neutrons.

References

[1] N.N. Ajitanand. Calculation of the effects of electronic threshold and pulse height walk on observed neutron time-of-flight distribution. *Nuclear Instruments and Methods*, 176:545–547, 1980.

[2] L.G. Chiang, R.B. Oberer, and S.A. Pozzi. Method to correlate CFD discriminator level and energy deposition by neutrons and photons in a fast plastic scintillating detector. Technical Report ORNL/TM-2000/193, Oak Ridge National Laboratory, 2000.

[3] M. Drosg, D.M. Drake, and P. Lisowski. The contribution of carbon interactions to the neutron counting efficiency of organic scintillators. *Nuclear Instruments and Methods*, 1980.

[4] H. Gotoh and H. Yagi. Solid angle subtended by a rectangular slit. *Nuclear Instruments and Methods*, 96:485–486, 1971.

[5] K. Gul. A study of neutron detection efficiency of an organic scintillation detector through simulation of detection processes. *Nuclear Instruments and Methods*, 176:549–554, 1980.

[6] Glenn F. Knoll. *Radiation Detection and Measurement*, pages 119–120. John Wiley & Sons, Inc., 2nd edition, 1989.

[7] J.T. Mihalczo, J.A. Mullens, J.K. Mattingly, and T.E. Valentine. Physical description of nuclear materials identification system (NMIS) signatures. *Nuclear Instruments and Methods*, 450:531–555, August 2000.